

Studies on scleroglucan conformation by rheological measurements *versus* temperature up to 150°C

C. Noïk* and J. Lecourtier

Institut Français du Pétrole, BP 311, 92506 Rueil-Malmaison, France

(Received 10 July 1991; revised 10 April 1992)

A newly designed viscometer was used to measure the viscosity of polymer solutions under high-temperature and low-shear-rate conditions. Rheograms of dilute and concentrated scleroglucan solutions were determined in the range of temperatures between 30 and 150°C. Rheological behaviour was correlated with macromolecule structural parameters. Intrinsic viscosity values *versus* temperature were analysed on the basis of Yamakawa's theory of semirigid chains. As the temperature increased, local molecular rigidity decreased. An Arrhenius equation form was found for the persistence length variation *versus* temperature. An apparent activation energy of 7.5 kJ mol⁻¹ (1.8 kcal mol⁻¹) was determined. This value was of the same order of magnitude as the hydrogen bond energy that stabilizes the scleroglucan triple-helix structure. On considering a model of rod particles, the scleroglucan molecule behaves like a rod-like polymer up to 130°C.

(Keywords: scleroglucan; conformation; rheology; temperature; viscosity; persistence length)

INTRODUCTION

Scleroglucan is a viscosifying non-ionic polysaccharide that appears to be an attractive additive for various applications. Among these are drilling fluids and improved oil recovery in the petroleum industry, and thickener fluids in the pharmaceutical industry.

The conformation in solution of scleroglucan and schizophyllan, another microbial polymer with a very similar chemical structure, has been extensively studied¹⁻⁹, especially by Yanaki. The polymer conformation is a semirigid chain made up of three helix strands associated by hydrogen bonds⁴ at ambient temperature and in an aqueous neutral solution. This structure gives local chain rigidity similar to that of xanthan polysaccharide, which also has a structure consisting of helix strands. A conformational change occurs and the polymer chain takes on a single-chain random-coil conformation in solution⁵ as the temperature increases or in an organic solvent.

Several structural studies by proton n.m.r. or X-ray diffraction^{6,7} have argued for the existence of these triple-helix strands. Light scattering diffusion measurements performed in a mixed solvent (water/dimethylsulphoxide) have determined a ratio of 3 between the molecular weights of the ordered and disordered forms⁸. This structural transition occurs at 135°C, and is due to the triple helices melting into single chains⁹. The thermal transition is irreversible and pH-dependent.

In this study, a newly designed viscometer was used in order to determine the rheograms of diluted and concentrated polymer solutions in a temperature range of 30 to 150°C. Rheological behaviour was correlated

with the structural parameters of the macromolecule at several temperatures, and was analysed by considering models of a semirigid-rod molecule.

EXPERIMENTAL

Polymer characteristics and preparation of solutions

The scleroglucan used is manufactured by Sanofi Bio Industries (France). Polymer broth is dissolved in brine (20 kg m⁻³ sodium chloride) by stirring gently overnight. To prevent any microbial contamination, 0.4 kg m⁻³ of sodium azoture bactericide is added to the solvent. Impurities with low molecular weight (lower than $M_w = 20\,000$), such as multivalent ions or residual fermentation molecules (glucose, proteins), are eliminated by extensive ultrafiltration. Then the macromolecules in solution are completely disaggregated by an appropriate heat treatment at 90°C. The protein impurities that remain linked to the chain are destroyed by denaturation during this treatment. The residual protein impurities have been measured by a specific spectrofluorometric method¹⁰. The measurements indicate that less than 1% by weight of proteins compared with scleroglucan molecules stay in solution.

It has been verified¹¹ by measuring various structural parameters that the scleroglucan chain is not degraded during this treatment. The intrinsic viscosity and molecular weight remain unchanged during the process, and the Huggins constant k' alone decreases. This means that polymer-polymer interactions in solution become lower than polymer-solvent interactions.

The main solution properties of improved scleroglucan have already been published: filterability experiments show that no microgels remain in solution¹²; viscosity measurements done over a long period in a strictly

* To whom correspondence should be addressed

controlled atmosphere indicate that the polymer solutions are stable and have no problem of aggregation with time¹³.

Polymer concentrations are determined with a Dohrman carbon organic analyser with an accuracy of 2%.

Oxygen is eliminated from the solutions by bubbling extrapurified nitrogen through them in order to prevent any chemical degradation during flow experiments at high temperature. The final oxygen content was less than 5 ppb (parts per billion: 10^{-9}), which is the detection limit for the CHEMets® tests (CHEMetrics).

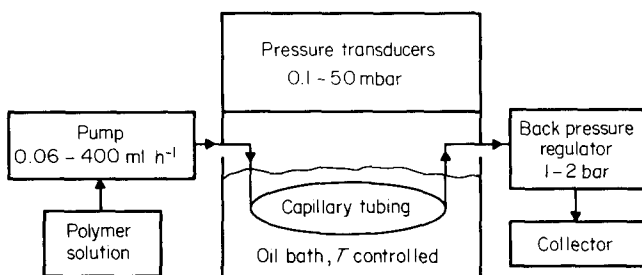
Viscosity measurements at different temperatures

Viscosity was measured at 30°C with a Contraves Low-Shear apparatus. For higher temperatures it was necessary to use a specially designed capillary viscometer based on the measurement method proposed by Liauh and Liu¹⁴. The viscometer was appropriately equipped so that accurate measurements could be obtained for low-viscosity fluids over a wide range of shear rates, including very low ones, up to 150°C. The first results with this viscometer have been presented previously¹⁵.

High-temperature/low-shear viscometer

Experimental principle. This is based on pressure-drop measurements at a controlled temperature across a very long capillary through which polymer solutions flow at a constant flow rate Q . A schematic representation of the viscometer is given in Figure 1. Calibrated nickel tubes were used for the capillaries in order to prevent any corrosion or metallic contamination of the solution. The capillary tubes were heated in an oil bath, where the temperature was strictly controlled to an accuracy of 0.1%. The syringe pump used (Iscot) delivered very stable flow rates between 10^{-11} m³ s⁻¹ (0.06 ml h⁻¹) and 10^{-7} m³ s⁻¹ (400 ml h⁻¹).

Different capillary lengths L and inner radii r were taken to establish the rheological curves for shear rates between 0.01 and 10 000 s⁻¹. Consequently, in the studied range of concentrations, the broad range of shear rates investigated allows the polymer solutions to exhibit Newtonian as well as pseudo-plastic behaviours. Pressure transducers able to measure pressure drops as low as 10^{-5} Pa or 1 mbar, for example, were used for dilute polymer solutions, where viscosity and measured pressure drop are low.



Capillary tubing characteristics
 Tubing in nickel metal
 Length = 5.0 - 17.2 m
 Inner radius = 0.5 - 1.1 × 10⁻³ m
 Shear rate range = 0.01 - 10000 s⁻¹

Figure 1 Schematic diagram of the lower-shear/high-temperature viscometer

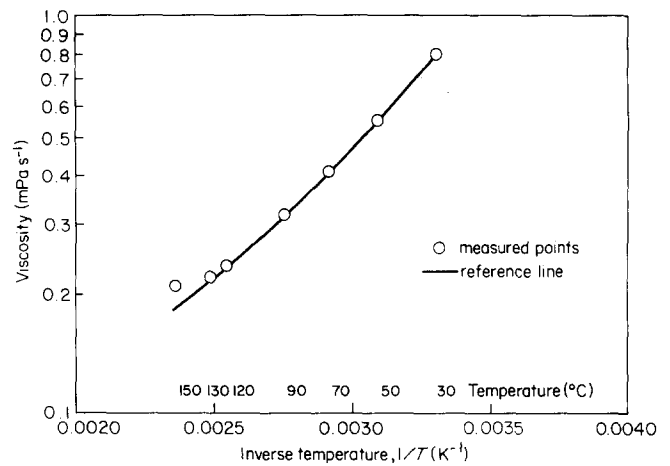


Figure 2 Viscometer calibration with brine solution

Viscometer calibration and feasibility. Viscosity measurements on brine solutions at 30 and 130°C were found to differ by less than 1% from measurements reported in the literature¹⁶ (Figure 2). Comparative experiments at 30°C on the Contraves apparatus gave the same viscosity value, with an experimental accuracy of 2% for the two methods used. The flow remained laminar at the maximum flow rate used, as the calculated Reynolds number was less than 100. The pressure drop due to entrance effects was negligible since the length to radius ratio of the tubes was very large ($L/r = 34\,400$ or 4527). Moreover, the curvature to capillary radius ratio was sufficiently high to prevent any secondary flow effects.

The results obtained agreed well when the viscosity was evaluated in different capillary geometries. So, effects such as inaccessible pore volume or viscoelastic behaviour in a narrow constriction can be considered negligible for the polymer solution.

Viscosity measurements. After temperature stabilization, the pressure drop was measured at a determined flow rate. All the apparatus has been proven safe, i.e. no oxygen entry was detected, so polymer macromolecules were not degraded thermally during the experiments. For temperatures over 90°C, it was necessary to work with a back-pressure regulator with a pressure drop around 10^{-2} Pa (1-2 bar) in order to stay in the liquid phase.

The shear stress τ is deduced from the flow relation:

$$\text{polymer: } \tau_p = (r/2L)\Delta P_p \quad (1)$$

$$\text{solvent: } \tau_s = (r/2L)\Delta P_s \quad (2)$$

where ΔP_p is the pressure drop during polymer solution flow, and ΔP_s that of solvent flow.

The shear rate γ is deduced from the value of flow rate Q , and calculated at the tube wall by using the Rabinovitch equation:

$$\text{polymer: } \gamma_p = [(3n + 1)/4n]4Q/\pi r^3 \quad (3)$$

$$\text{solvent: } \gamma_s = 4Q/\pi r^3 \quad (4)$$

where n is the log derivative of the shear stress function versus flow rate:

$$n = d \ln \tau_p / d \ln (4Q/\pi r^3) \quad (5)$$

n is equal to 1 for a Newtonian fluid and is shear-rate-dependent for a non-Newtonian fluid. However, a wide class of polymeric fluids show power-law behaviour over

a large range of shear rates. In the power-law region, n is constant and lower than 1 for a pseudo-plastic fluid. So n is calculated directly from a logarithmic plot of pressure ΔP_p versus flow rate Q :

$$n = d \ln \Delta P_p / d \ln Q \quad (6)$$

By definition, the steady shear viscosity is the shear stress to shear rate ratio:

$$\text{polymer: } \eta_p = \tau_p / \dot{\gamma}_p \quad (7)$$

$$\text{solvent: } \eta_s = \tau_s / \dot{\gamma}_s \quad (8)$$

Relative viscosity η_r , defined as the polymer solution to brine viscosity ratio, is related to the ratio $\Delta P_p / \Delta P_s$ as follows:

$$\eta_r = \eta_p / \eta_s = [4n / (3n + 1)] \Delta P_p / \Delta P_s \quad (9)$$

So pressure-drop measurements were made at several flow rates for polymer and brine solutions at the same temperature. The measurements can be used to evaluate the relative viscosity of polymer solutions at different shear rates. Note that this relation is also valid if n is not constant.

The relative viscosity $\eta_{r,0}$ corresponding to the Newtonian viscosity $\eta_{p,0}$ of the polymer solutions is expanded in a Taylor series:

$$\eta_{r,0} = \eta_{p,0} / \eta_s = 1 + [\eta]_0 C_p + k' ([\eta]_0)^2 C_p^2 + \dots \quad (10)$$

where $[\eta]_0$ is the Newtonian intrinsic viscosity, k' the Huggins constant and C_p the polymer concentration. The Newtonian intrinsic viscosity $[\eta]_0$, which is equivalent to the inverse of a concentration, is related to the conformation in solution of the isolated polymer chain.

According to equation (10), the Newtonian intrinsic viscosity $[\eta]_0$ is defined by the limiting value at zero polymer concentration of the reduced specific viscosity η_{rsv} , which is equal to $(\eta_{r,0} - 1) / C_p$:

$$[\eta]_0 = \lim_{C_p \rightarrow 0} (\eta_{rsv}) = \lim_{C_p \rightarrow 0} [(\eta_{r,0} - 1) / C_p] \quad (11)$$

To determine the intrinsic viscosity at zero shear rate, the relative viscosity at the Newtonian plateau $\eta_{r,0}$ is measured for several polymer concentrations in the dilute domain. It is considered that the low-concentration domain is reached when the overlap parameter defined by $C_p [\eta]_0$ is less than 1. The experiments were run within the limits $C_p [\eta]_0$ of 0.01 to 1.0.

Intrinsic viscosity is related to conformation in solution and the molecular weight of the macromolecule. The Huggins constant k' is calculated from the intrinsic viscosity value and the slope b of the curve of the reduced specific viscosity η_{rsv} variation versus polymer concentration C_p :

$$k' = b / ([\eta]_0)^2 \quad (12)$$

The constant k' is correlated with the solution properties of polymer molecules. A theoretical value of around 0.4 is expected for macromolecules in good solvent conditions without any specific interactions with other molecules.

RESULTS AND DISCUSSION

Intrinsic viscosity versus temperature

Viscosity was measured at different temperatures. Viscosity values under Newtonian conditions were used to determine relative viscosity $\eta_{r,0}$. The variations in the Newtonian reduced specific viscosity versus polymer

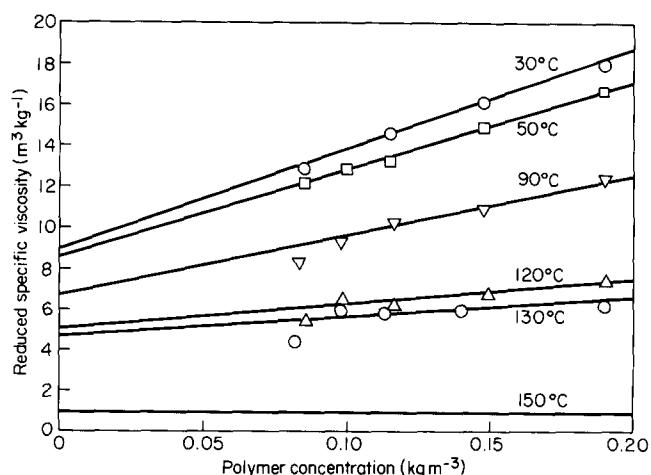


Figure 3 Variation in reduced specific viscosity versus polymer concentrations at different temperatures between 30 and 150°C in NaCl (20 kg m⁻³)

Table 1 Intrinsic viscosity $[\eta]_0$ and Huggins constant k' values versus temperature

Temperature (°C)	30	50	90	120	130	150
$[\eta]_0$ (m ³ kg ⁻¹)	9.20	8.50	6.70	4.80	4.60	0.85
k'	0.50	0.58	0.64	0.56	0.47	0.60

concentration at temperatures between 30 and 150°C are shown in Figure 3.

Values of intrinsic viscosity and the Huggins constant at the experimental temperatures are presented in Table 1.

Intrinsic viscosities obtained by extrapolating the reduced specific viscosity at zero polymer concentration decreased slightly with increasing temperature up to 120°C. Above 130°C, the drastic decrease observed was due to a thermally induced change in the scleroglucan structure. Measurements were made both ways (temperature increase and decrease), and showed that the viscosity change is reversible up to 120°C. Above 130°C, the thermal transition is irreversible.

The effect of time on the scleroglucan conformation transition was not studied; each measurement took about 30 min (1800 s). Note, however, that triple-helix denaturation kinetics can be expected to be dependent on solvent salinity conditions.

The Huggins constant characterizing intermolecular interactions in solution did not vary between 30 and 150°C within experimental errors. The brine solution remained a good solvent for scleroglucan even at high temperatures for dilute polymer solutions. No attractive interactions occurred.

Yanaki established the same relation between the intrinsic viscosity and molecular weight for the two polysaccharides, schizophyllan and scleroglucan¹⁻⁴, at 25°C in aqueous solution with 0.01 mol m⁻³ sodium hydroxide. In water, where the polysaccharide macromolecules are in triple-helix form, the power-law relation is:

$$[\eta]_0 \propto M_w^{1.8} \quad \text{for } M_w < 5 \times 10^5 \quad (13)$$

$$[\eta]_0 \propto M_w^{1.1} \quad \text{for } M_w > 10^6 \quad (14)$$

An exponent value of 1.8 is the theoretical prediction for a rigid-rod conformation. Yanaki suggested that a polymer with high molecular weight behaves more like

a semirigid chain than a strictly rigid rod¹⁷ for the lower value of 1.1.

The characteristics of our polymer at 30°C, i.e. an intrinsic viscosity of 9.2 m³ kg⁻¹ and a molecular weight of 5 × 10⁶, determined by light scattering, were consistent with Yanaki's experimental curve. When the rigid structure of scleroglucan is broken at 150°C, an intrinsic viscosity of 0.85 m³ kg⁻¹ was measured.

Scleroglucan conformation versus temperature

The intrinsic viscosity–molecular weight dependence was established by Yamakawa and Fujii by using a worm-like cylinder model for stiff chains with no excluded volume¹⁸:

$$[\eta]_0 = \Phi L_c^{3/2} / (\lambda^3 M_w) \quad (15)$$

The main parameters in this relation are the following:

(i) The Kuhn statistical length λ^{-1} , which is the persistence length q multiplied by 2:

$$\lambda^{-1} = 2q \quad (16)$$

(ii) The contour length L_c and the reduced contour length L_r , defined by:

$$L_r = \lambda M_w / M_L = \lambda L_c \quad (17)$$

with the mass per unit length M_L , which is the ratio of the molecular weight M_0 to the length of the monomer unit h :

$$M_L = M_0 / h \quad (18)$$

(iii) The Flory constant Φ , which depends on L_r .

The term d_r is the reduced hydrodynamic diameter, which is related to the hydrodynamic diameter d :

$$d_r = \lambda d \quad (19)$$

Variations of Φ as a function of L_r and d_r are shown in tables in ref. 18.

It is impossible to determine q , M_L and d from the intrinsic viscosity alone. The literature^{4,17} gives average M_L and d values of around 2200 nm⁻¹ and 3 nm, for schizophyllan and scleroglucan polymers, respectively. So, we can calculate the persistence length for each studied temperature with these values, with the different intrinsic viscosity determinations and a given molecular weight equal to 5 × 10⁶. Final results are presented in Table 2.

We calculated a persistence length of 145 nm at 30°C, which is close to the value of around 180 ± 30 nm estimated by Kashiwagi *et al.* for schizophyllan in water at 25°C¹⁹.

Table 2 Intrinsic viscosity $[\eta]_0$ and persistence length q values versus temperature

Temperature (°C)	30	50	90	120	130
$[\eta]_0$ (m ³ kg ⁻¹)	9.20	8.50	6.70	4.80	4.60
q (nm)	145	135	108	80	75

Table 3 Persistence length q ratio versus temperature

Temperature (°C)	30	50	90	120	130
$q(T)/q(30^\circ\text{C})$	1	0.90	0.82	0.74	0.55

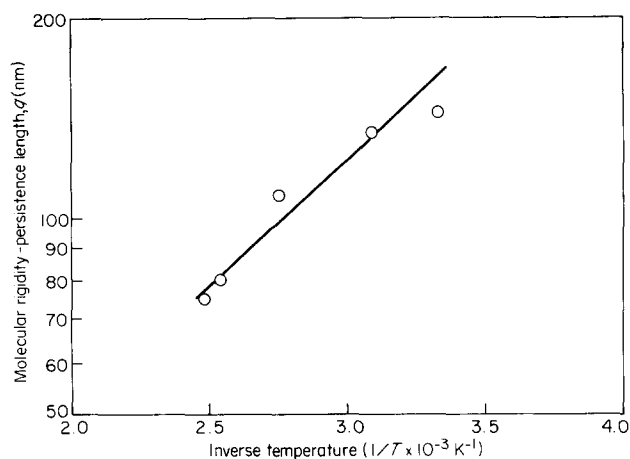


Figure 4 Temperature effects on scleroglucan molecular rigidity

As the temperature increases, local molecular rigidity decreases. The triple-helical scleroglucan structure is stabilized by interchain hydrogen bonds owing to the presence of hydroxy groups in the glucose unit. The increase in macromolecular chain flexibility is mainly due to the decrease in the energy of hydrogen bonds versus temperature.

Intrinsic viscosity was determined several times, and all the experiments are summarized in Table 3, where the persistence length at the studied temperature T was divided by the reference taken at 30°C.

A linear relation was established between the logarithmic value of the persistence length ($\log q$) and the inverse temperature in kelvins ($1/T$) (Figure 4):

$$\log q \propto \Delta H_a / RT \quad (20)$$

This Arrhenius equation form was used to calculate an apparent activation energy (ΔH_a) of 7.5 kJ mol⁻¹ (1.8 kcal mol⁻¹), which is similar to the hydrogen-bond energy, i.e. 4.2–8.4 kJ mol⁻¹ (1–2 kcal mol⁻¹). In the range of values investigated, intrinsic viscosity and persistence length values can be considered proportional. Therefore, the activation energy value is the same for the two Arrhenius equation forms with temperature:

$$[\eta]_0 \propto q$$

so

$$[\eta]_0 = A \exp(\Delta H_a / RT) \quad (21)$$

with

$$A = 0.50 \pm 0.05 \text{ m}^3 \text{ kg}^{-1}$$

Viscosity and shear-rate behaviour versus temperature

The relative viscosity of scleroglucan solutions versus shear rate is plotted in log–log coordinates in Figures 5, 6 and 7 at different temperatures. The classical Rabinovitch correction presented in equations (3) and (4) was used for shear-rate and viscosity determinations. As usually found for pseudo-plastic polymer solutions, all the curves are of the same shape whatever the concentration values. The curves show a Newtonian regime where the viscosity $\eta_{r,0}$ is independent of shear rate, followed by a plastic regime where the viscosity η_r decreases versus shear rate according to a power law. The transition area is characterized by critical shear rate $\dot{\gamma}_c$. The critical point is equal to the inverse of relaxation time θ , which is

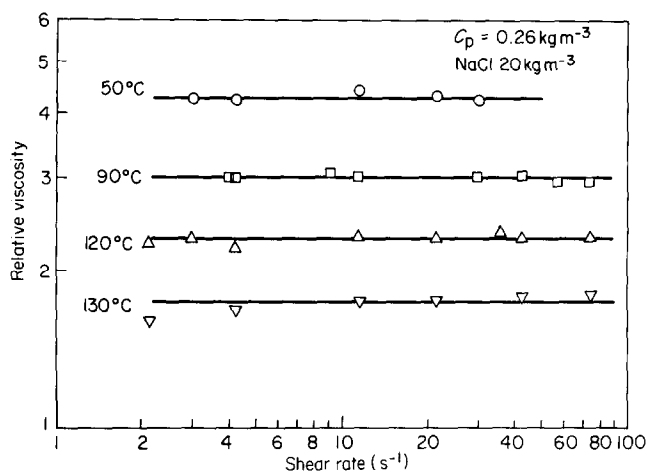


Figure 5 Relative viscosity versus shear rate of scleroglucan solution (0.260 kg m^{-3}) in NaCl (20 kg m^{-3}) at different temperatures

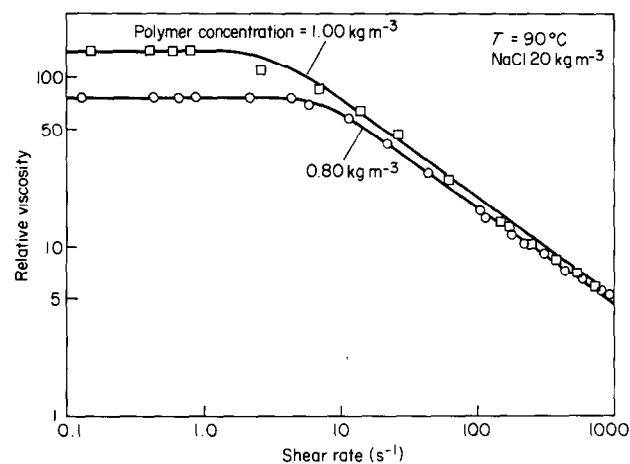


Figure 6 Relative viscosity versus shear rate of scleroglucan solutions in NaCl (20 kg m^{-3}) at 90°C

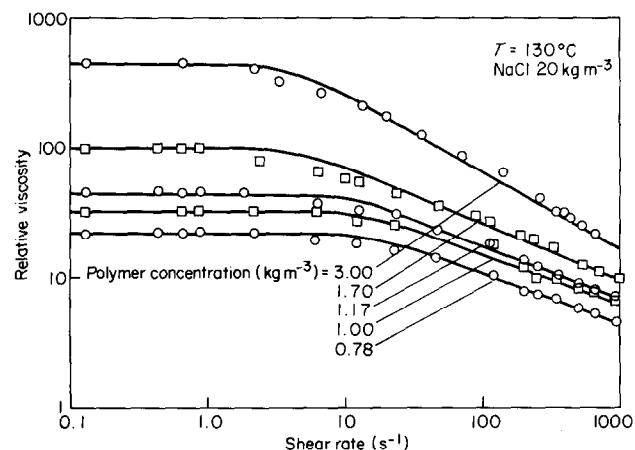


Figure 7 Relative viscosity versus shear rate of scleroglucan solutions in NaCl (20 kg m^{-3}) at 130°C

considered as a characteristic of the scleroglucan macromolecule behaviour in solution. The solution behaved like a Newtonian fluid between 0.5 and 100 s^{-1} in the semidilute domain for a polymer concentration of 0.26 kg m^{-3} (Figure 5), whatever the temperature between 50 and 130°C . Rheological curves are presented in Figures 6 and 7 for more concentrated solutions at 90 and 130°C . It should be noted that the experimental points deduced from the two capillaries fit together very well.

Newtonian regime. Newtonian viscosity decreases with temperature. Before the scleroglucan structural thermal change, the viscosity decrease may be expressed by an Arrhenius form of equation with an activation energy ΔH_b , whatever the polymer concentration:

$$\log \eta_r = B + (\Delta H_b / RT)$$

with B and ΔH_b functions of C_p .

For each concentration, the apparent activation energy was determined from the slope of plots of viscosity versus inverse temperature expressed in kelvins. The results are presented in Figure 8 and summarized in Table 4.

The variation in activation energy versus concentration is plotted in log-log coordinates in Figure 9. Two different concentration domains can be observed: a dilute one where the chains are not entangled, and a semidilute one where the chains begin to overlap each other. A limit concentration C_{lim} of around 0.20 kg m^{-3} was determined from these measurements.

At concentrations below C_{lim} , the logarithmic value of the activation energy varies linearly with concentration with a slope of around 2.1 ± 0.1 . Above C_{lim} , the variation is smoother and the slope of the curve is around 0.8 ± 0.1 .

This limit concentration C_{lim} appeared to be very close to the concentration usually called C^* , which indicates the beginning of the semidilute regime. However, C_{lim} seemed to be independent of temperature. This can be

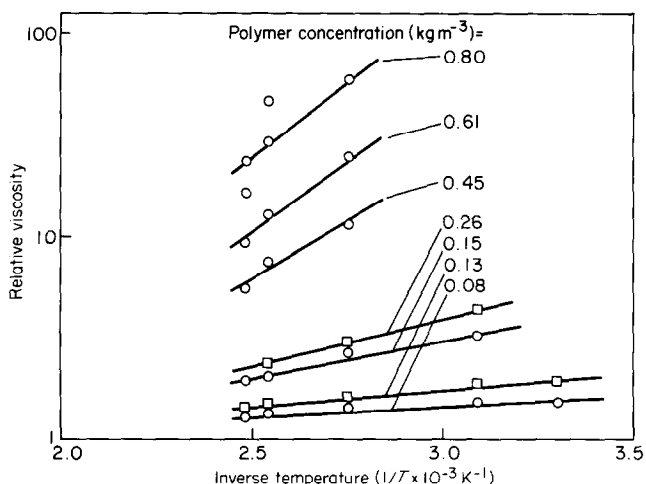


Figure 8 Variation in relative Newtonian viscosity versus temperature of scleroglucan solutions in NaCl (20 kg m^{-3})

Table 4 Activation energy ΔH_b values versus polymer concentration C_p ($\log \eta_r = B + \Delta H_b / RT$)

C_p (kg m^{-3})	0.08	0.13	0.15	0.19	0.26	0.45	0.46	0.61	0.80	0.98	1.40
ΔH_b (kcal mol^{-1})	0.5	0.9	1.6	2.4	2.2	6.8	5.0	6.8	8.0	10	12

$1 \text{ kcal mol}^{-1} = 4.18 \text{ kJ mol}^{-1}$

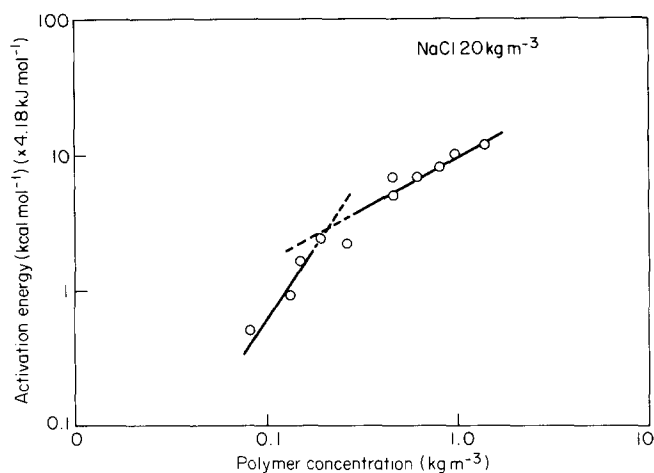


Figure 9 Variation in activation energy versus polymer concentration

explained within experimental errors by the polydispersity of our polymer sample. Moreover, competitive effects on the variation of C^* versus temperature can be expected. Scleroglucan polymer considered as a semirigid chain has a behaviour in solution between a rod molecule and a flexible chain. In the first case, concentration C^* decreases with the length of the rod; and in the second case, C^* increases when the local rigidity of the molecule decreases.

Values of the activation energy ΔH_b varied between one and ten times the value of the H-bond energy. In the first part of this paper, activation energy ΔH_a was determined from intrinsic viscosity variation. It is of the same order of magnitude as the H-bond energy.

The two energies were correlated according to the relative viscosity definition. As a preliminary approximation:

$$\eta_r = 1 + [\eta]_0 C_p \quad (22)$$

and

$$[\eta]_0 = A \exp(\Delta H_a/RT)$$

from equation (21), so:

$$\log \eta_r = \log[1 + C_p A \exp(\Delta H_a/RT)] \quad (23)$$

(i) For $AC_p \exp(\Delta H_a/RT) < 1$, i.e. in dilute conditions, for low values of C_p and if $\Delta H_a/RT$ is negligible, $\Delta H_a/RT \ll 1$, then:

$$\log[1 + AC_p \exp(\Delta H_a/RT)] \approx AC_p \exp(\Delta H_a/RT) \quad (24)$$

and

$$\exp(\Delta H_a/RT) \approx 1 + \Delta H_a/RT$$

so

$$\log \eta_r = AC_p + AC_p \Delta H_a/RT \quad (25)$$

So apparent activation energy ΔH_b must correspond to $AC_p \Delta H_a$, and varies linearly with concentration C_p . This is what we observed experimentally. But the values of $\Delta H_a/RT$ are between 3 at 30°C and 2 at 130°C in the range of temperature investigated. So the first assumption is not realistic.

(ii) On the contrary, if $AC_p \exp(\Delta H_a/RT) > 1$, then:

$$\begin{aligned} \log \eta_r &= \log[AC_p \exp(\Delta H_a/RT)] \\ \log \eta_r &= \log(AC_p) + \Delta H_a/RT \end{aligned} \quad (26)$$

So the logarithmic value of relative viscosity now varies linearly with inverse temperature with the same slope whatever the concentration. The apparent activation energy is independent of concentration. But this was not observed experimentally, particularly at high polymer concentrations.

In fact, it seems that the two theoretical assumptions considered correspond to the two polymer concentration conditions.

(i) Apparent activation energy drastically increases with polymer concentration in the dilute concentration condition, and is of the same order of magnitude (Table 4) as the H-bond energy. Energy variation at low concentrations may correspond to breaking of the intramolecular bonds in one macromolecular chain in solution, and also, with less sensitivity, to the intermolecular bonds between chains.

(ii) Above C_{lim} , the energy is greater (about 10 times the hydrogen-bond energy) and increases with concentration with a lower slope. In semidilute solutions, polymer-polymer interactions are mainly dependent on the intermolecular bond energy between one chain and another, and on the number of contacts between chains, which increases with the polymer volume fraction. Moreover, the scleroglucan structure is maintained by hydrogen bonds. Above the fusion temperature, aggregation of single chains was observed by Yanaki⁴. Interactions leading to chain aggregation phenomena can be expected at temperatures close to the critical one.

This can explain the high values of activation energy versus concentration; both inter- and intramolecular bonds are disrupted as the temperature increases.

Shear-thinning regime. The experimental points were fitted with Carreau's model²⁰ where relative viscosity at a given shear rate is deduced from relaxation time and Newtonian viscosity $\eta_{r,0}$. Infinite viscosity is assumed to be one:

$$(\eta_r - 1)/(\eta_{r,0} - 1) = [1 + (\theta\dot{\gamma})^2]^{-m} \quad (27)$$

Values of the power-law exponent $2m$ and relaxation time deduced at various polymer concentrations and temperatures are presented in Table 5. The Carreau exponent $2m$ increases with polymer concentration, and for the same viscosity value it decreases when the temperature increases. As expected, relaxation time increases with polymer concentration or fractional free-volume occupancy. The variation in relaxation time is linear versus polymer concentration, at 130°C on log-log coordinates, as shown in Figure 10. The points are well described by a slope of 2.5 at 90°C.

The variation in relaxation time versus polymer concentration in the semidilute concentration domain, i.e. for an overlap parameter $C_p[\eta]_0$ range from 1 to 5, for xanthan solutions in brine has been studied by several

Table 5 Relative viscosity $\eta_{r,0}$, Carreau's exponent $2m$ and relaxation time θ values versus polymer concentration at 90 and 130°C

Temperature	90°C				130°C			
	C_p (kg m ⁻³)							
	1.00	0.78	2.60	1.70	1.17	1.00	0.78	
$\eta_{r,0}$	140	73	440	98	45	32	22	
$2m$	0.59	0.61	0.62	0.49	0.41	0.40	0.38	
θ (s)	0.26	0.14	0.19	0.12	0.09	0.07	0.06	

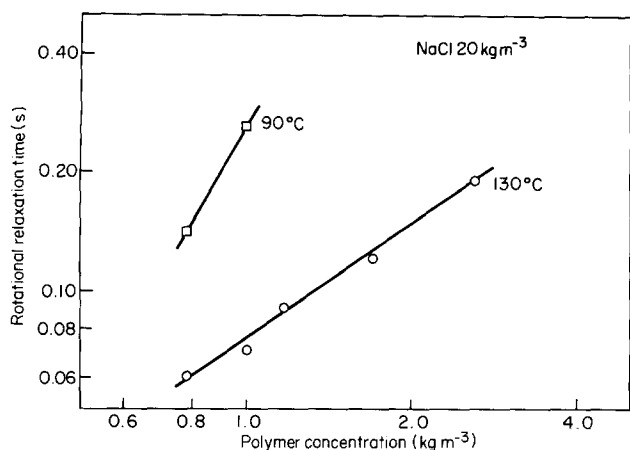


Figure 10 Relaxation time variation *versus* polymer concentration at 90 and 130°C

Table 6 Comparison between experimental and calculated diffusion constant D values

Temperature (°C)	Experimental			Calculated			
	θ_0 (s)	D (s ⁻¹)	$[\eta]_0$ (m ³ kg ⁻¹)	p	L_{rod} (nm)	d_{rod} (nm)	D (s ⁻¹)
90	11.3×10^{-3}	44	6.70	490	1470	2.86	36
130	9.3×10^{-3}	54	4.60	395	1180	3.03	84

authors. Allain²¹ determined a slope of 2.0 at 30°C and Cuvelier²² measured a slope of 2.1 at 25°C. Moreover, the length of the equivalent rod particle of scleroglucan molecule at 90°C is of the same order of magnitude as that of a xanthan molecule. These remarks suggested that scleroglucan behaves like a semirigid macromolecule at 90°C.

The extrapolation of relaxation time θ_0 at zero polymer concentration gives values of around 0.01 s at 90 and 130°C. Relaxation time can be estimated from a diffusion constant D by using the expression established from a rigid rod:

$$\theta_0 = 1/(2D) \quad (28)$$

Diffusion constant D is dependent on length L_{rod} and diameter d_{rod} of the equivalent rod particle considered²³:

$$D = (3kT/\pi\eta_s L_{rod}^3) [\ln(2L_{rod}/d_{rod}) - a] \quad (29)$$

A relationship was determined, assuming that the molecule behaves like a strictly rigid rod, between intrinsic viscosity and a factor p . This factor is the length to diameter ratio ($p = L_{rod}/d_{rod}$) for $50 < p < 2000$ ²⁴:

$$[\eta]_0/V_{sp} = 0.159p^{1.8} \quad (30)$$

where V_{sp} is the specific volume, equal to 0.620 for oligosaccharides. Then length L_{rod} is calculated from p , intrinsic viscosity $[\eta]_0$ and molecular weight M_w (ref. 19):

$$L_{rod}^3 = (45/2\pi N_A) [\eta]_0 M_w [\ln(2p) - a] \quad (31)$$

where N_A is Avogadro's number and a is a correction factor taken to be equal to 0.8.

Determination of experimental values of $[\eta]_0$ at 90 and 130°C is presented in Table 1. The final results of experimental and calculated values are given in Table 6 for the two temperatures studied.

Whatever the temperature, the calculated value of

equivalent diameter d_{rod} of the rod is constant and close to values ($d = 2.6 \pm 0.4$ nm) found in the literature⁴. The correlation between experimental and calculated D values is quite satisfactory within experimental errors at 90°C. It is similar to the value ($D = 45$ s⁻¹) found for a xanthan molecule with the double-helix configuration²⁵.

The decrease in length of the equivalent rod and the increase in diffusion constant at higher temperatures indicated an increase in chain flexibility with temperature.

Viscosity and polymer concentration versus temperature

The variations in relative Newtonian viscosity *versus* polymer concentrations are presented in Figure 11 at 90, 120 and 130°C. Polymer viscosity was measured in 20 kg m⁻³ sodium chloride solvent and in reconstituted sea-water brine.

Whatever the temperature, viscosities increased with polymer concentrations and were independent of solvent quality. As expected for a non-ionic polysaccharide, multivalent ions had no effect on the rheological behaviour of scleroglucan solutions.

After a transition zone (C_p greater than C^*) viscosity variations *versus* polymer concentration follow a power law on log-log coordinates. The value of the slope is 3.1 ± 0.1 at 90°C and slightly decreases with temperature to 2.3 ± 0.1 at 130°C.

The variation of the slope of viscosity *versus* polymer concentration was calculated by Doi and Edwards²³ to be 3 for a rigid-rod molecule and assumed to be around 2 for flexible chains.

Scleroglucan behaviour *versus* temperature indicated that polymer properties are similar to those of a semirigid chain at 90°C, and the molecule behaves like a flexible chain at 130°C.

CONCLUSIONS

The newly designed capillary viscometer was used to study the rheological behaviour of scleroglucan solutions over a wide range of shear rates at temperatures up to 150°C.

A linear relation was established between the logarithmic value of the persistence length and the inverse temperature, according to Yamakawa's theory and intrinsic viscosity values. This Arrhenius equation form

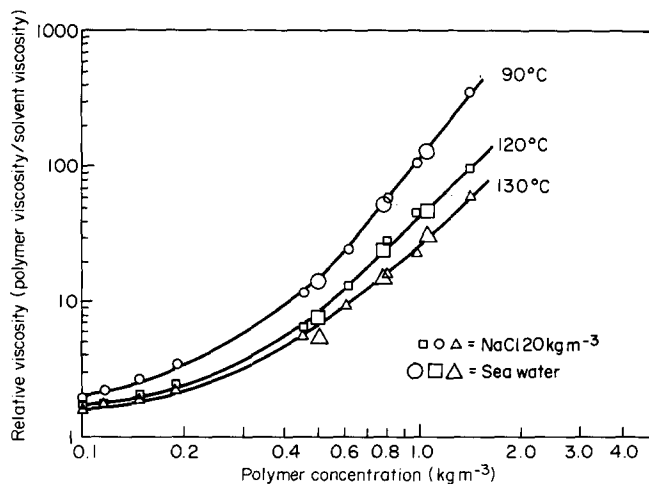


Figure 11 Relative viscosity *versus* scleroglucan concentration at different temperatures in NaCl (20 kg m⁻³) or sea water

was used to calculate an apparent activation energy of 7.5 kJ mol^{-1} ($1.8 \text{ kcal mol}^{-1}$). This energy is similar to the energy of the hydrogen bonds that maintain the multi-stranded structure of the molecule.

In the semidilute domain of polymer concentrations, rotational relaxation time decreased, and then the rotational diffusion constant increase was correlated to an increase in chain flexibility *versus* temperature.

ACKNOWLEDGEMENTS

The authors would like to thank E. Praet for performing experiments. We are grateful to C. Allain for her advice and comments on this manuscript.

REFERENCES

- 1 Yanaki, T., Kojima, T. and Norisuye, T. *Polym. J.* 1981, **13**, 1135
- 2 Itou, T., Teramoto, A., Matsuo, T. and Suga, H. *Macromolecules* 1986, **19**, 1234
- 3 Nardin, R. and Vincendon, M. *Macromolecules* 1989, **22**, 3551
- 4 Yanaki, T. and Norisuye, T. *Polym. J.* 1983, **15**, 389
- 5 Sato, T., Norisuye, T. and Fujita, H. *Carbohydr. Res.* 1981, **95**, 195
- 6 Rinaudo, M. and Vincendon, M. *Carbohydr. Polym.* 1982, **2**, 135
- 7 Bluhm, T. L., Deslandes, Y., Marchessault, R. H., Perez, S. and Rinaudo, M. *Carbohydr. Res.* 1982, **100**, 117
- 8 Norisuye, T., Yanaki, T. and Fujita, H. *J. Polym. Sci.* 1980, **18**, 547
- 9 Yanaki, T., Tabata, K. and Kojima, T. *Carbohydr. Polym.* 1985, **5**, 275
- 10 Jones, B. N., Pääbo, S. and Stein, S. *J. Liq. Chromatogr.* 1981, **4**, 565
- 11 Noik, C., Lecourtier, J. and Chauveteau, G., ACS, Div. Polym. Mater., Proc., New Orleans, 1987, Vol. 57, pp.380-4
- 12 Lecourtier, J., Noik, C., Barbey, P. and Chauveteau, G., 4th Eur. Symp. on Enhanced Oil Recovery, Proc., DGMK, Hamburg, 1987, pp.105-16
- 13 Rivenq, R., Donche, A. and Noik, C., SPE 19635, 64th Annual Technical Conference and Exhibition, San Antonio, Texas, 8-11 October 1989, pp.775-84
- 14 Liauh, W. W. and Liu, T. W. SPE 12649, 58th Annual Technical Conference and Exhibition, San Francisco, California, 5-8 October 1983
- 15 Noik, C., Lecourtier, J., Rivenq, R. and Donche, A., European Oil and Gas Conference, Palermo, Sicily, Italy, Proc. 9-12 October 1990, p. 206
- 16 Swindwells, J. F., 'National Bureau of Standards, Handbook of Chemistry and Physics', 63rd Edn. (Eds. R. C. Weast and M. J. Astle), 1983, F-40
- 17 Yanaki, T., Norisuye, T. and Fujita, H. *Macromolecules* 1980, **13**, 1462
- 18 Yamakawa, H. and Fujii, M. *Macromolecules* 1974, **7**, 128
- 19 Kashiwagi, Y., Norisuye, T. and Fujita, H. *Macromolecules* 1980, **14**, 1220
- 20 Carreau, P. J., Bui, Q. H. and Leroux, P. *Rheol. Acta* 1979, **5**, 18
- 21 Allain, C., Lecourtier, J. and Chauveteau, G. *Rheol. Acta* 1988, **27**, 255
- 22 Cuvelier, G. and Launay, B., IX Int. Congress on Rheology, Mexico, 1984, p. 247
- 23 Doi, M. and Edwards, S. F. in 'The Theory of Polymer Dynamics', Clarendon Press, Oxford, 1988, p.295
- 24 Layec, Y. and Wolff, C. *Rheol. Acta* 1974, **13**, 696
- 25 Chauveteau, G. *J. Rheol.* 1982, **26**, 111

NOMENCLATURE

a	Correction factor
A, B	Experimental coefficients
b	Slope of the curve η_{rsv} <i>versus</i> C_p
C_p	Polymer concentration
C_{lim}	Limit concentration
C^*	Semidilute concentration regime
D	Diffusion constant
d	Hydrodynamic diameter of the molecule
d_r	Reduced hydrodynamic diameter
d_{rod}	Diameter of the rod
$\Delta H_a, \Delta H_b$	Apparent activation energies
h	Length of monomer unit
k	Boltzmann constant
k'	Huggins constant
L	Capillary length
L_c	Contour length
L_r	Reduced contour length
L_{rod}	Length of the rod
M_L	Mass per unit length
M_0	Mass of monomer unit
M_w	Molecular weight
$2m$	Carreau exponent
N_A	Avogadro's number
n	Slope of the curve ($\ln \tau$ polymer) <i>versus</i> ($\ln Q$)
ΔP	Pressure drop
p	Length to diameter ratio of the rod
q	Persistence length
Q	Flow rate
R	Gas constant
r	Capillary inner radius
T	Temperature
V_{sp}	Specific volume of polymer
γ	Shear rate
η_p	Polymer viscosity
$\eta_{p,0}$	Newtonian polymer viscosity
η_s	Solvent viscosity
η_r	Relative viscosity
$\eta_{r,0}$	Newtonian relative viscosity
η_{rsv}	Reduced specific viscosity
$[\eta]_0$	Newtonian intrinsic viscosity
θ	Relaxation time
θ_0	Relaxation time at zero polymer concentration
λ^{-1}	Kuhn statistical length
τ	Shear stress
Φ	Flory constant